

Reconfiguration of PV Arrays (T-C-T, B-L, H-C) Considering Wiring Resistance

Kandipati Rajani and Tejavathu Ramesh[✉], *Senior Member, IEEE*

Abstract—Partial shadings on the photovoltaic (PV) array causes reduction in maximum power generation. Reconfiguration of PV arrays plays an important role in increasing the maximum power generation from PV array configurations under partial shadings. In general, partial shadings on the PV arrays are concentrated on a group of modules. Therefore, the distribution of shading over the array increases the maximum power generation. This paper uses a modified Sudoku pattern to increase the maximum power generation from the PV array configurations. The PV array configurations are analyzed by considering column wiring resistance and cross ties resistance. The modified Sudoku pattern is applied to Total-Cross-Tied (T-C-T), Bridge-Link (B-L) and Honey-Comb (H-C) configurations and their performances are analyzed under various shading patterns, such as short narrow, short wide, long narrow, long wide, middle and diagonal. The specifications, such as Global Maximum Power (GMP), Mismatch losses, Fill Factor, Efficiency are considered to see the efficacy of various PV array configurations and their reconfigurations. From the results, it can be concluded that reconfigured T-C-T PV array generates the highest GMP compared to other configurations under considered shading patterns.

Index Terms—Bridge-link, efficiency, fill factor, global maximum power, honey-comb, photovoltaic array, reconfiguration, Sudoku, Total-Cross-Tied.

I. INTRODUCTION

THE effective electricity supply is one of the important factors in economic growth of any country. In the 1950 s, India implemented a program for supporting economic growth and enhancing the quality of life by electrifying the rural areas [1]. The demand of renewable energy sources increases day by day due to the shortage of fossil fuels and global warming. Among all the renewable energy sources, solar energy is plentiful in nature and free of pollution [2], [3]. By installing photovoltaic (PV) generation systems, solar energy can be converted into electrical energy. Therefore, it can be helpful in upgrading the agriculture, education, healthcare and domestic sectors etc. [4].

Extraction of maximum power from PV systems is an important task, even when there is no change in irradiance.

Maximum power can be extracted from PV systems by using Maximum Power Point techniques (MPPT), such as Perturb & Observe, Incremental conductance etc. [5]. All the conventional MPPTs are efficient if and only if one maximum power point is present in Power-Voltage (P-V) curves. Sometimes multiple peaks present in P-V curves damaged panels and partial shadings on panels with bypass diodes. The partial shadings on PV panels are generally due to poles, trees, other PV panels, buildings, dust, bird's droppings and passing clouds, etc. The irradiance on PV systems is not constant throughout the day due to partial shadings [6]. Shaded PV modules behave like resistors and will consume the energy of nearby modules. Therefore, heat will be generated from shaded module and this effect is called hotspot on the PV module. By using bypass diodes, this problem can be resolved, but multiple peaks on P-V curves happen due to these bypass diodes under shading. Multiple peaks in PV curves reduce the efficiency of PV systems. Therefore, under partial shading to track the Global Maximum Power (GMP) point, various AI and Hybrid MPPT techniques have been proposed [7], [8]. The problems involved in identifying the GMP under partial shadings are reported in [9]. The advanced MPPT methods give accurate tracing of the GMP point. But these methods are costly and require complex control arrangements. Professional skills are required to create a greater number of parameters [10].

Partial shadings on PV panels causes mismatch losses. The differences between maximum powers generated under standard test conditions and partial shading conditions are called mismatch losses. These losses are proportional to the pattern of shading, configuration of the PV array and the position of the shaded panel in an array. To minimize the mismatch losses, various array configurations are listed in literature [11], [12]. Series (S), Series-Parallel (S-P), Bridge-Link (B-L) and Honey-Comb (H-C) are compared under different shading patterns and it has been concluded, that the H-C configuration is superior to the remaining three in [13]. In [14] modeling and performance of various PV array configurations (S, P, S-P, B-L, H-C and T-C-T) under various partial shadings were analyzed. It was observed from the results that the T-C-T configuration performs better in terms of producing maximum power and a lesser number of LMP points. Comparison of different PV array configurations were carried out in [15] and it was concluded that Total-Cross-Tied (T-C-T), B-L and H-C configurations reduce mismatch losses compared with a S-P configuration. However, the reduction is low in the case of B-L and H-C configurations than in the case of a T-C-T configuration. In [16] various array configurations

Manuscript received December 25, 2020; revised April 6, 2021; accepted July 26, 2021. Date of online publication May 6, 2022; date of current version June 17, 2022.

K. Rajani and T. Ramesh (corresponding author, e-mail: tramesh.ee@nit andhra.ac.in; ORCID: <https://orcid.org/0000-0002-2687-369X>) are with the Electrical and Electronics Engineering Department, National Institute of Technology Andhra Pradesh, West Godavari-534101, India.

DOI: 10.17775/CSEEJPES.2020.06930

are compared under different shading patterns and it was concluded that anti parallel bypass diodes to the panel are mandatory under partial shading. In most of the shading patterns, T-C-T generates the highest GMP, except in some shading patterns, such as the number of columns receiving the same irradiance is more than the number of rows. In this case, H-C configuration generates the highest GMP because of less ties [17]. In [18], a novel Triple-Tied-Cross-Linked (T-T-C-L) PV array configuration was proposed with a reduced number of cross ties to enhance the maximum power. A novel fixed PV array configuration was proposed in [19] to harvest the maximum power from the PV array with reduced number of cross ties. In [20], Alternate Total Cross Tied - Bridge Linked (A-TCT-BL) PV array configurations were modeled and compared with S, S-P, H-C, T-C-T and B-L. A current source in each row of the 4X4 T-C-T PV array was considered and analyzed in [21].

Further, improvement of GMP under partial shading can be obtained by changing the architecture of the system and reconfiguration of the PV arrays. Changing system architecture means changing the inverter [22] and converter topologies [23], [24]. By using different electrical row currents, equalizing the generated currents is called the reconfiguration of the PV arrays [25]. Reconfiguration methods are primarily classified into static and dynamic reconfigurations. Dynamic reconfiguration sensors are used to detect the partially shaded PV panel and switches are used to change the electrical interconnection of the PV array [26]–[28]. Static reconfiguration physical locations of PV modules are changed without effecting its electrical connection. In the static method, there is no need of additional equipment, such as switches, sensors and monitoring devices for switching control. In [29], a Sudoku puzzle based rearrangement of PV panels for T-C-T was proposed and it analyzed the performance of the PV array under different shading patterns. An optimized Sudoku based configuration was proposed in [30] by considering mutual shadow patterns on T-C-T PV arrays. This method has high complexity in construction. An Improved Sudoku configuration for a T-C-T PV array was proposed in [31] to improve GMP under various shading patterns. An odd-even structure of static reconfiguration was used for enhancement of maximum power from the PV array in [32]. In [33], a novel Magic-Square puzzle PV array reconfiguration was proposed. In [34], a Sudoku puzzle reconfiguration was applied to a hybrid BL-TCT PV array configuration. A zig-zag static reconfiguration was proposed in [35] to distribute the shading throughout the array instead of for a single column. The drawback of the zig-zag technique is complex in construction and more wiring is required. In Sudoku and optimal Sudoku reconfiguration techniques, the first column modules are not distributed. Therefore, shading on the first column modules remains undistributed. In [36], a Modified Sudoku reconfiguration pattern was proposed for a 9×9 T-C-T PV array. In this paper, by considering Cross ties resistance and column wiring resistance, the performance analysis of various PV array configurations (B-L, H-C and T-C-T) using a Modified Sudoku reconfiguration was done.

The remainder of this paper is organized as follows: Section II describes the mathematical modeling of the PV array

and array configurations; Section III presents reconfiguration of the PV array, calculation of column wiring resistance and cross ties resistance; Results and discussions are presented in Section IV and Section V concludes this paper.

II. DESCRIPTION OF PV SYSTEM

A. Mathematical Modeling of PV Module

A PV module is formed by connecting PV cells in series. In general, a PV cell is modeled with a current source in parallel with a diode [37], [38]. The equivalent circuit of the PV cell is represented in Fig. 1. R_{sh} is the shunt resistance, it carries leakage current and R_s , which is the series resistance, it carries the terminal current of the PV cell. The terminal current of the PV cell can be represented by (1).

$$I_{cell} = I_{L,cell} - I_D \left[\exp \left(\frac{V_{cell} + R_s I_{cell}}{V_T a} - 1 \right) \right] - \frac{V_{cell} + R_s I_{cell}}{R_{sh}} \quad (1)$$

where $I_{L,cell}$ is the photo current generated, I_{cell} is the terminal current of the PV cell, I_D is the saturation current, V_{cell} is the terminal voltage of the PV cell, $V_T = KT/q$, is the thermal voltage of the PV cell, “ k ” is the Boltzmann’s constant, “ T ” is the temperature of PV cell, “ q ” is the charge of electron and “ a ” is the ideality factor.

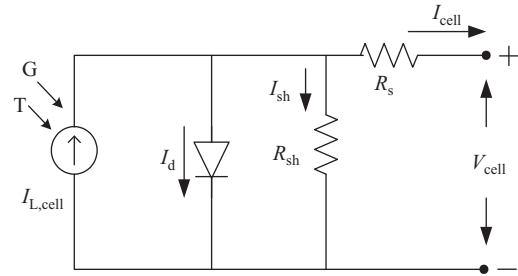


Fig. 1. PV cell equivalent circuit.

If the n_s number of the PV cells are connected in series in a PV module, then the terminal current of the PV module (1) is obtained by modifying (1).

$$I = I_L - I_D \left[\exp \left(\frac{q(V + R_S I)}{n_s k T a} - 1 \right) \right] - \frac{V + R_S I}{R_{SH}} \quad (2)$$

where R_S and R_{SH} are the series and shunt resistance of the PV module, I_L is the photo current generated from the PV module and it generally depends on solar insolation or irradiance and temperature on the PV module. It is represented by (3).

$$I_L = \frac{G}{G_o} [I_{L,SO} + K_{SO}(T_C - T_o)] \quad (3)$$

where K_{SO} is the module temperature coefficient under the standard test condition (STC), $I_{L,SO}$ is the generated current under standard solar irradiance G_o (1000 W/m^2) and standard temperature T_o (25°C).

B. PV Array Configurations

To obtain the required amount of voltage, the number of modules is connected in series and it is called a string. To obtain that required amount of current, the number of strings are connected in parallel and it is called a PV array. Several types of PV array configurations are listed in literature [11]–[21]. Among all the configurations, three important configurations are considered as shown in Fig. 2. During partial shading conditions, the shaded module comes under overheating conditions. To protect the module from overheating, bypass diodes are connected antiparallel to the PV modules. A diode is connected in series to each string in an array to avoid the reversal of current. In a PV array, all the modules are interconnected in a bridge architecture form, then the array is called a Bridge-Link (B-L) configuration. This configuration can be represented as shown in Fig. 2(a). If all the modules are connected in a honey comb structure or hexogen shape as shown in Fig. 2(b), it is called a Honey-Comb (H-C) configuration. If all modules in strings are cross-tied, then the connection is called a Total- Cross-Tied (T-C-T). Output voltage (V_j), current (I_j) and power (P_o) of this PV array are:

$$V_o = \sum_{j=1}^9 V_{j1} = V_{11} + V_{21} + V_{31} + \dots + V_{91} = 9V_j \quad (4)$$

$$I_o = \sum_{j=1}^9 I_{1j} = I_{11} + I_{12} + I_{13} + \dots + I_{19} = 9I_j \quad (5)$$

$$P_o = 81V_j I_j \quad (6)$$

III. RECONFIGURATION OF PV ARRAY

A. Modified Sudoku Reconfiguration Pattern

To extract the maximum power from the PV array, a modified sudoku reconfiguration pattern [38] as shown in Fig. 3(b) is used in this paper. A modified sudoku pattern is obtained by using the following steps: 1) first consider the partially filled

5	4		7					2	51	42	93	34	75	16	67	88	29	1	7	3	5	8	0	4	6	2
	3			4				9	11	32	83	24	45	66	77	58	99	1	1	1	4	5	7	1	2	2
		7	9					1	21	62	73	94	55	86	47	38	19	3	5	2	1	4	3	3	6	3
6			5					7	61	92	13	54	25	46	87	78	39	1	1	1	8	6	1	6	3	3
4	7			8					41	72	23	64	85	36	17	98	59	4	8	2	5	1	3	5	4	2
									31	82	53	14	95	76	27	48	69	3	6	3	1	4	5	7	6	1
			8						71	22	33	84	65	56	97	18	49	3	2	6	3	6	4	1	4	3
									91	12	43	74	35	26	57	68	89	2	1	1	1	4	3	2	3	1
									81	52	63	44	15	96	37	28	79	1	2	1	4	1	6	3	4	6
5	6																	2	6	9	7	4	1	3	5	8

(a)

(b)

(c)

Fig. 3. (a) Partially filled Sudoku puzzle. (b) Modified Sudoku Reconfiguration pattern. (c) Multiplication factor table of column wiring resistance.

Sudoku puzzle as shown Fig. 3(a). 2) Then apply the recursive back tracking algorithm [36]. This algorithm allots the 1 to 9 numbers in unfilled cells and then checks whether there is any number repeats in the row, column and 3×3 grids or not. 3) If yes, it will go for back tracking, otherwise it will go to recursive checking for unfilled cells till all cells are filled.

To analyze the performance of PV array configurations (B-L, H-C, T-C-T) using the modified sudoku pattern, six shading patterns have been considered. Considered shadings are: short narrow, short wide, long narrow, long wide, middle and diagonal shadings as shown in Figs. 5, 6, 7, 8 respectively. Depending on the shaded number of rows and columns and the number of modules shaded per row and column, shading patterns are defined [13], [14].

B. Column Wiring Resistance Calculation

KYOCERA-KC200GT PV module of size 1.425 m \times 0.99 m is considered for the PV array. The continuous arrangement is taken for modules in a column as shown in Fig. 4(a). The wiring arrangement of column 1 and column 2 of the modified Sudoku reconfiguration are shown in Fig. 4(a). The I_{sc} of each PV module is 8.21 A and therefore, in a column to connect the modules in series, the wire must have an ampacity of $1.56 \times I_{sc} = 12.8$ A as per National Electrical Code (NEC) [40]. For the ampacity of 12.8 A, 16 AWG (American Wire Gauge) wires are used and the resistance per km wire length is 13.2 ohm. Wire covering the length of one

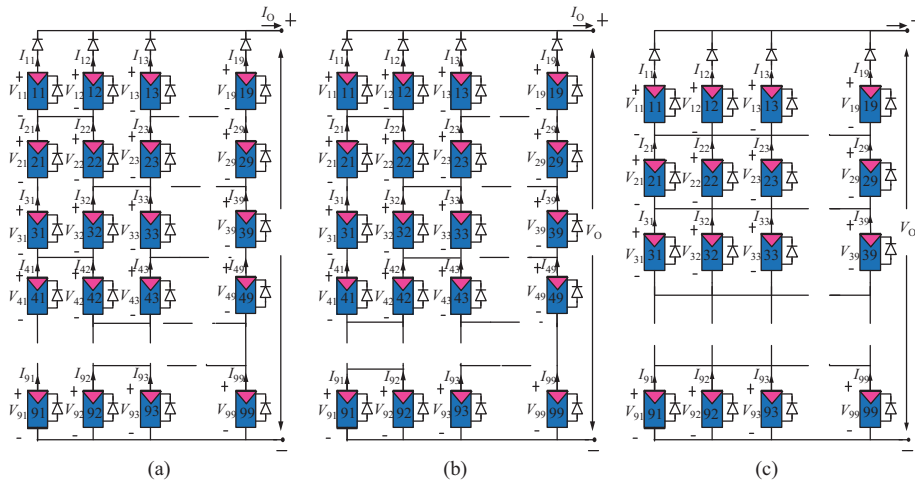


Fig. 2. The 9×9 PV arrays connected in: (a) Bridge-Link, (b) Honey-Comb, and (c) Total-Cross-Tied.

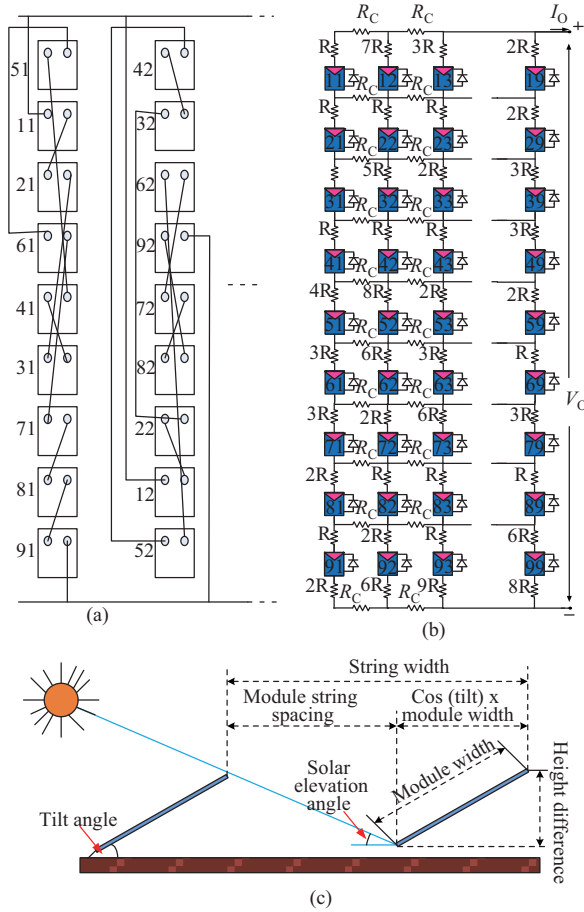


Fig. 4. (a) Modified Sudoku reconfiguration wiring diagram of column 1 and column 2. (b) Circuit for Modified Sudoku reconfiguration. (c) Representation of PV string width calculation.

module has a resistance $R = 0.0132 \times 1.425 = 0.0187$ ohms. The multiplication factor for R is shown in Fig. 3(b). By multiplying resistance R with the numbers in the multiplication factor table, it will determine the column resistance of the wire inbetween the modules. Module-11 is rearranged by one row and for the wire required for connecting to the positive terminal, the wire has to cover one module length and its resistance is R . When module-12 is arranged next to module-11, the wire has to cover one module length. Therefore, the resistance of the wire required for connecting the module-11 negative terminal to the positive terminal of module-12 is R . To connect the negative terminal of module-12 to the positive module-13, the wire has to cover three modules. Therefore, the length of the wire having resistance is $3R$. Module-16 is placed in its original position only and the positive terminal of module-16 is directly connected to the positive terminal of an array, and the resistance of the wire which covers the length is $0R$. In a similar way, the entire multiplication factor table is formed. The circuit connection of the 9×9 T-C-T PV array as per the modified Sudoku reconfiguration, by including the column wiring resistance and cross ties resistance, is shown in Fig. 4(b).

C. Cross Ties Resistance Calculation

To determine the cross ties resistance, spacing between

strings [41] was considered as shown in Fig. 4(c). String Width can be calculated as:

$$\text{String Width} = \text{Minimum Module String Spacing} + \text{Cos (Tilt Angle)} \times \text{Module Width}$$

Where, Minimum Module String Spacing = Module String Spacing \times Cos (Azimuth Correction Angle), Module String Spacing = Height Difference / Tan (solar elevation angle), Height Difference = Sin (Tilt Angle) \times Module Width.

For 15° tilt angle and 0.99 m module width, the height difference of the module is 10 inches. If we consider 17° of the solar elevation angle and 44° Azimuth Correction angle for the calculation of the Module String Spacing and Minimum Module String Spacing, then the value is 33 inches and 24 inches respectively. String width is 1.5748 m for a module width of 0.99 m. Therefore, the length of the wire required for cross ties is 1.5748 m, and the crossties resistance is $R_C = 0.0132 \times 1.5748 = 0.0207$ ohms.

IV. RESULTS AND DISCUSSION

For the performance analysis of the proposed Sudoku reconfiguration, the PV array configurations T-C-T, B-L, H-C under different shading patterns was considered. By using measures, such as GMP [42], mismatch losses, fill factor and efficiencies, the effectiveness of the proposed method was analyzed. The KYOCERA-KC200GT PV module was used in MATLAB/Simulink for modeling and simulation of PV array configurations. The parameters of the PV module are given in Table I in the appendix. The mismatch losses of a PV array can be calculated by (7).

$$\text{Loss} = \frac{P_{mu} - P_{mps}}{P_{mu}} \times 100 \quad (7)$$

where P_{mps} is the global maximum power under PSCs and P_{mu} is the maximum power at uniform irradiance. For a PV module, maximum current and voltage are the short circuit current (I_{sc}) and open circuit voltage (V_{oc}). For practical purposes, the power generated from the PV module is zero at these operating points. Maximum power from the solar cell can be determined by using the Fill Factor (FF), which is the ratio of the maximum power to the product of V_{oc} and I_{sc} .

$$FF = \frac{V_{mp} \times I_{mp}}{V_{oc} \times I_{sc}} \times 100 \quad (8)$$

TABLE I
PV MODULE DATA AND MODEL PARAMETERS

S. no.	Parameters	Values
1	Maximum power: P_m	200.143 W
2	Current at maximum power point: I_{mp}	7.61 A
3	Voltage at maximum power point: V_{mp}	26.3 V
4	Short circuit current: I_{SC}	8.21 A
5	Open circuit voltage: V_{OC}	32.9 V
6	Temperature co-efficient of I_{SC} : K_I	0.0032 A/K
7	Temperature co-efficient of V_{OC} : K_V	-0.1230 V/K
8	Diode emission coefficient: 'a'	1.3
9	PV module dimensions (Area)	1425 mm \times 990 mm
10	Cells per module: n_s	54
11	Shunt resistance, R_{SH}	603.4349 Ω
12	Series resistance, R_S	0.2318 Ω

where V_{mp} is the voltage at maximum power and I_{mp} is the current at maximum power generated by the PV array. The efficiency of a PV module depends on the spectrum, intensity of the incident sunlight and the temperature [43] of the PV module. Therefore, efficiency (η) is defined as the ratio of maximum power generated to the solar power input to panels.

$$\eta = \frac{V_{mp} \times I_{mp}}{I \times A} \times 100 \quad (9)$$

where A is the area of the PV array on which solar irradiance falls and I is the solar irradiance per unit area.

A. Short Narrow Shading (SN)

In SN shading, a lesser number of modules in a row and column are shaded; five groups of modules shaded with 0.3 kW/m², three group of modules shaded with 0.7 kW/m² and the remaining seventy three group of modules are shaded with 1 kW/m² as shown in Fig. 5. The PV curves of T-C-T, B-L, H-C configurations and reconfigurations under short narrow shading are shown in Fig. 6. From the results, it can be observed that the highest GMP of 14,013.76 W is generated by reconfigured T-C-T by considering wiring losses (column wiring resistance and cross ties resistance losses). It can be observed from Table II that the T-C-T configuration has 570.19 W and 535.12 W enhancement in generated power when compared to the B-L and H-C configurations. Reconfigured T-C-T has 975.7 W and 1236.34 W improvement in generated power than the reconfigured B-L and H-C configurations. Reconfigured T-C-T, along with wiring losses, has 730.47 W and 759.23 W improvement in generated power when compared to the reconfigured B-L and

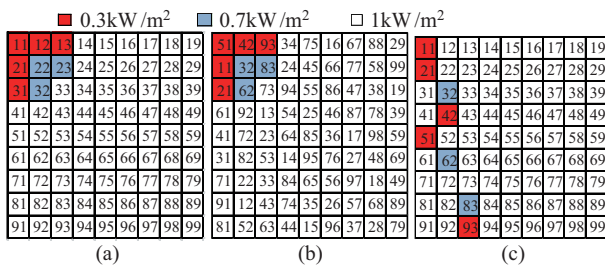


Fig. 5. Short narrow shading on: (a) 9 × 9 PV array, (b) Reconfigured 9 × 9 PV array, and (c) Shading dispersion by Sudoku.

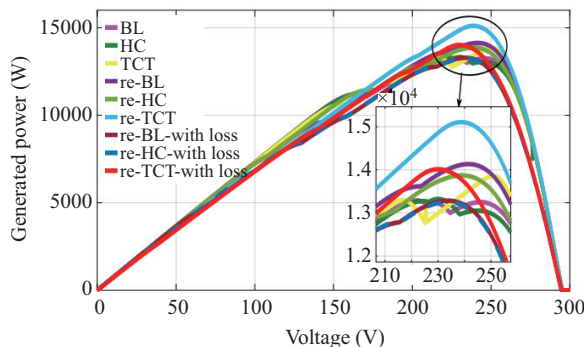


Fig. 6. Comparison of PV curves of T-C-T, B-L, H-C configuration and reconfigurations under SN shading.

TABLE II

PERFORMANCE ANALYSIS SPECIFICATIONS UNDER SN SHADING

Configurations	P_{mp}	ML (%)	FF (%)	η (%)
B-L	13288.07	17.78	60.74	11.63
H-C	13323.14	17.57	60.90	11.66
T-C-T	13858.26	14.26	63.42	12.13
re-BL	14132.81	12.56	64.67	12.37
re-HC	13872.05	14.17	63.48	12.14
re-TCT	15108.48	6.52	69.22	13.22
re-B-L-with loss	13283.29	17.81	60.79	11.62
re-H-C-with loss	13254.53	17.99	60.66	11.60
re-T-C-T-with loss	14013.76	13.29	66.50	12.26

H-C configurations. Therefore, wiring losses in reconfigured B-L, H-C, T-C-T are 849.52 W, 617.52 W and 1,094.72 W respectively. Reconfigured T-C-T has the least mismatch losses of 6.52% without considering wiring losses. There are 13.29% mismatch losses in the T-C-T reconfiguration by considering wiring losses. The 12.6% highest efficiency was obtained by reconfigured T-C-T with wiring losses.

B. Short Wide Shading (SW)

In SW shading, seven columns out of nine columns are shaded, six rows out of nine rows are shaded and no row and column are completely shaded. Therefore, this type of shading is called short wide shading. Seven groups of modules are shaded with 0.3 kW/m², eight group of modules are shaded with 0.5 kW/m², fourteen group of modules are shaded with 0.7 kW/m², twelve group of modules are shaded with 0.9 kW/m² and the remaining thirty nine group of modules are shaded with 1 kW/m² as shown in Fig. 7. The PV curves of T-C-T, B-L, H-C configurations, and reconfigurations under short wide shading are shown in Fig. 8. From the results, it can be observed that the highest GMP of 12,766.08 W was generated by reconfigured T-C-T by considering wiring losses (column wiring resistance and cross ties resistance losses). It can be observed from Table III that the T-C-T configuration has 589.08 W and 635.02 W enhancements in generated power when compared to the B-L and H-C configurations. Reconfigured T-C-T has 1,219.4 W and 1,479.12 W improvement in generated power than the reconfigured B-L and H-C configurations. Reconfigured T-C-T, along with wiring losses, has 1,120.81 W and 1,402.07 W improvement in generated power than the reconfigured B-L and H-C configurations. Therefore, wiring losses in reconfigured B-L, H-C, T-C-T are 551.69 W, 573.26 W and 650.31 W respectively. Reconfigured T-C-T has the least mismatch losses of 16.9% without considering

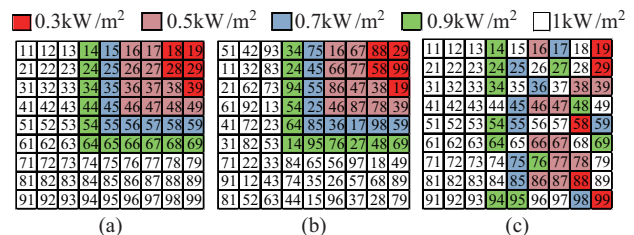


Fig. 7. Short wide shading on: (a) 9 × 9 PV array, (b) Reconfigured 9 × 9 PV array, and (c) Shading dispersion by Sudoku.

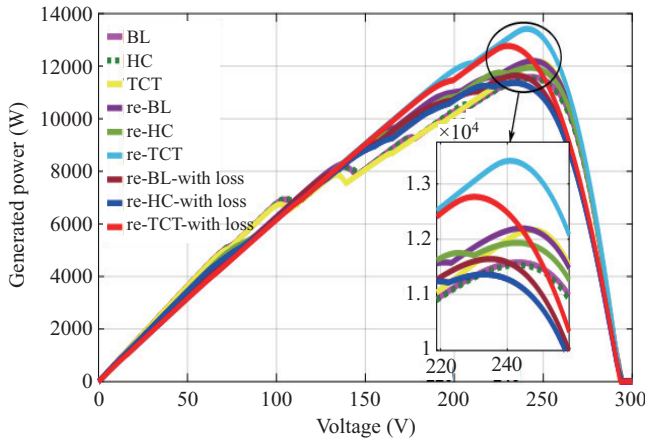


Fig. 8. Comparison of PV curves of T-C-T, B-L, H-C configuration and reconfigurations under SW shading.

TABLE III
PERFORMANCE ANALYSIS SPECIFICATIONS UNDER SW SHADING

Configurations	P_{mp}	ML (%)	FF (%)	η (%)
B-L	11581.46	28.34	53.23	10.14
H-C	11535.52	28.63	53.02	10.09
T-C-T	12170.54	24.70	55.95	10.65
re-BL	12196.96	24.54	58.96	10.67
re-HC	11937.27	26.14	56.27	10.45
re-TCT	13416.39	16.99	67.96	11.74
re-B-L-with loss	11645.27	27.95	56.52	10.19
re-H-C-with loss	11364.01	29.69	53.74	9.94
re-T-C-T-with loss	12766.08	21.01	64.92	11.17

wiring losses. There are 21.01% mismatch losses in the T-C-T reconfiguration when considering wiring losses. The 11.1% highest efficiency was obtained by the reconfigured T-C-T with wiring losses.

C. Long Narrow Shading (LN)

In LN shading, three columns out of nine columns are completely shaded, nine rows are shaded and no row is completely shaded. Therefore, this type of shading is called long narrow shading. Seven groups of modules are shaded with 0.3 kW/m², eight groups of modules are shaded with 0.5 kW/m², six groups of modules are shaded with 0.7 kW/m², six groups of modules are shaded with 0.9 kW/m² and the remaining fifty four groups of modules are shaded with 1 kW/m² as shown in Fig. 9. The PV curves of T-C-T, B-L, H-C configurations, and reconfigurations under Long Narrow shading are shown in Fig. 10. From the results, it can be observed that the highest GMP of 13,282.38 W was generated by the reconfigured T-C-T by considering wiring losses (column wiring resistance and cross ties resistance losses). It can be observed from Table IV that the T-C-T configuration has 386.21 W and 426.64 W enhancements in generated power when compared to the B-L and H-C configurations. Reconfigured T-C-T has 790.25 W and 823.3 W improvement in generated power than the reconfigured B-L and H-C configurations. Reconfigured T-C-T, along with wiring losses, has 668.54 W and 692.13 W improvement in generated power than the reconfigured B-L and H-C configurations. Therefore, wiring losses in reconfigured B-L, H-C, T-C-T are 471.44 W,

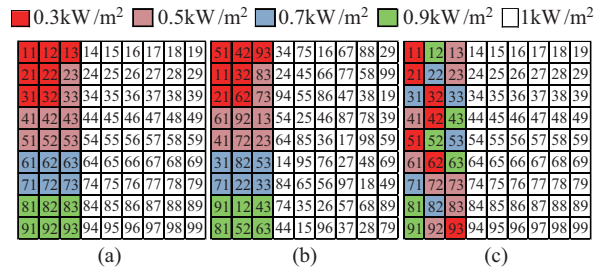


Fig. 9. Long Narrow shading on: (a) 9 × 9 PV array, (b) Reconfigured 9 × 9 PV array, and (c) Shading dispersion by Sudoku.

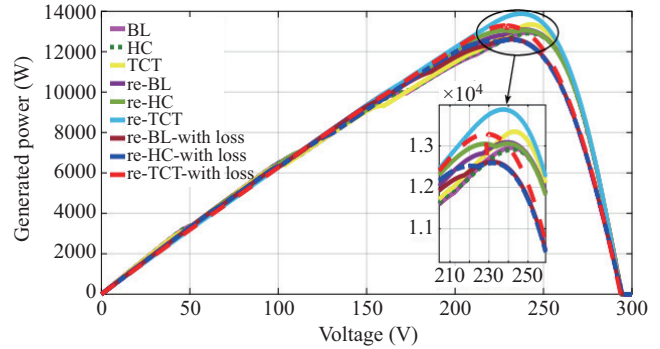


Fig. 10. Comparison of PV curves of T-C-T, B-L, H-C configuration and reconfigurations under LN shading.

TABLE IV
PERFORMANCE ANALYSIS SPECIFICATIONS UNDER LN SHADING

Configurations	P_{mp}	ML (%)	FF (%)	η (%)
B-L	12956.14	19.84	61.40	11.34
H-C	12915.71	20.09	61.14	11.30
T-C-T	13342.35	17.45	63.45	11.68
re-BL	13084.44	19.04	65.22	11.45
re-HC	13051.39	19.25	64.84	11.42
re-TCT	13874.69	14.15	70.88	12.14
re-B-L-with loss	12613.84	21.96	62.68	11.04
re-H-C-with loss	12590.25	22.10	62.49	11.02
re-T-C-T-with loss	13282.38	17.82	67.87	11.62

461.14 W, and 592.31 W respectively. Reconfigured T-C-T has the least mismatch losses of 17.82% without considering wiring losses. There are 14.15% mismatch losses in the T-C-T reconfiguration by considering wiring losses. The 11.62% highest efficiency was obtained by the reconfigured T-C-T with wiring losses.

D. Long Wide Shading (LW)

In LW shading, six columns out of nine columns are completely shaded, nine rows are shaded and no row is completely shaded. Therefore, this type of shading is called long wide shading. Eighteen groups of modules are shaded with 0.3 kW/m², eighteen groups of modules are shaded with 0.5 kW/m², nine groups of modules are shaded with 0.7 kW/m², nine groups of modules are shaded with 0.9 kW/m² and the remaining twenty seven groups of modules are shaded with 1 kW/m² as shown in Fig. 11. The PV curves of T-C-T, B-L, H-C configurations, and reconfigurations under long wide shading are shown in Fig. 12. From the results, it can be observed that the highest GMP of 10,681.36 W was

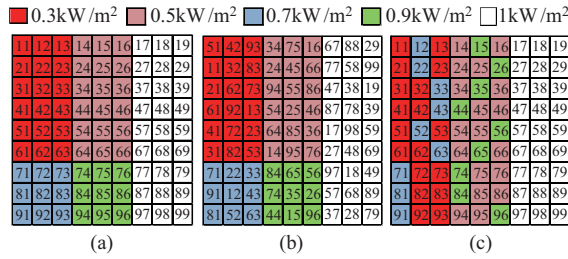


Fig. 11. Long wide shading on: (a) 9×9 PV array, (b) Reconfigured 9×9 PV array, and (c) Shading dispersion by Sudoku.

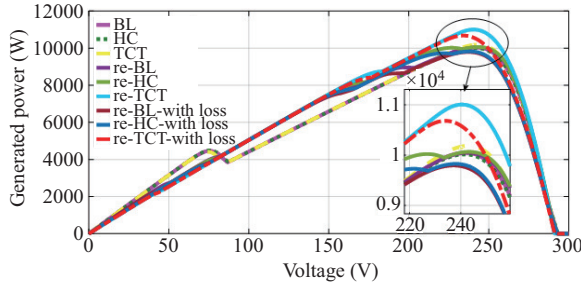


Fig. 12. Comparison of PV curves of T-C-T, B-L, H-C configuration, and reconfigurations under LW shading.

TABLE V
PERFORMANCE ANALYSIS SPECIFICATIONS UNDER LW SHADING

Configurations	P_{mp}	ML (%)	FF (%)	η (%)
B-L	10049.07	37.82	53.42	8.79
H-C	10115.12	38.03	53.12	8.76
T-C-T	10185.82	36.98	54.51	8.91
re-BL	10046.42	37.84	59.51	8.79
re-HC	10065.47	37.72	59.56	8.81
re-TCT	11005.35	31.91	69.61	9.63
re-B-L-with loss	9794.08	39.40	58.02	8.57
re-H-C-with loss	9826.04	39.20	58.15	8.60
re-T-C-T-with loss	10681.36	33.91	67.50	9.35

generated by the reconfigured T-C-T by considering wiring losses (column wiring resistance and cross ties resistance losses). It can be observed from Table V that the T-C-T configuration has 136.75 W and 170.7 W enhancements in generated power when compared to the B-L and H-C configurations. Reconfigured T-C-T has 958.93 W and 939.88 W improvement in generated power when compared to the reconfigured B-L and H-C configurations. Reconfigured T-C-T, along with wiring losses, has 887.28 W and 855.32 W improvement in generated power when compared to the reconfigured B-L and H-C configurations. Therefore, wiring losses in the reconfigured B-L, H-C, T-C-T are 252.34 W, 239.43 W, and 323.99 W respectively. Reconfigured T-C-T has the least mismatch losses of 33.91% without considering wiring losses. There are 31.91% mismatch losses in the T-C-T reconfiguration by considering wiring losses. The 9.35% highest efficiency was obtained by reconfigured T-C-T with wiring losses.

E. Middle Shading (M)

In M shading, the group of middle modules are shaded. Therefore, this type of shading is called middle shading. Four

groups of modules are shaded with 0.3 kW/m², four groups of modules are shaded with 0.5 kW/m², four groups of modules are shaded with 0.7 kW/m², four groups of modules are shaded with 0.9 kW/m² and the remaining sixty five groups of modules are shaded with 1 kW/m² as shown in Fig. 13. The PV curves of the T-C-T, B-L, H-C configurations, and reconfigurations under Middle shading are shown in Fig. 14. From the results, it can be observed that the highest GMP of 14,068.75 W was generated by the reconfigured T-C-T by considering wiring losses (column wiring resistance and cross ties resistance losses). It can be observed from Table VI that the T-C-T configuration has 378.69 W and 876.16 W enhancements in generated power when compared to the B-L and H-C configurations. Reconfigured T-C-T has 199.01 W and 708.81 W improvement in generated power when compared to the reconfigured B-L and H-C configurations. Reconfigured T-C-T, along with wiring losses, has 141.54 W and 581.63 W improvement in generated power when compared to the reconfigured B-L and H-C configurations. Therefore, wiring losses in reconfigured B-L, H-C, T-C-T are 599.75 W, 530.04 W, and 657.22 W respectively. Reconfigured T-C-T has the least mismatch losses of 12.95% without considering wiring losses.

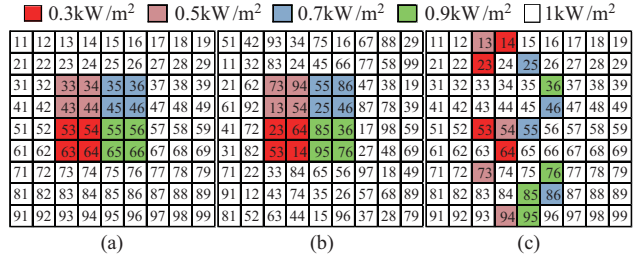


Fig. 13. Middle shading on: (a) 9×9 PV array, (b) Reconfigured 9×9 PV array, and (c) Shading dispersion by Sudoku.

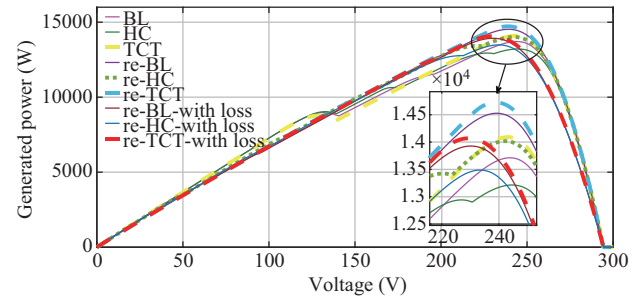


Fig. 14. Comparison of PV curves of T-C-T, B-L, H-C configuration, and reconfigurations under Middle shading.

TABLE VI
PERFORMANCE ANALYSIS SPECIFICATIONS UNDER M SHADING

Configurations	P_{mp}	ML (%)	FF (%)	η (%)
B-L	13712.22	15.16	62.82	12.00
H-C	13214.75	18.24	60.54	11.56
T-C-T	14090.91	12.82	64.63	12.33
re-BL	14526.96	10.12	66.63	12.71
re-HC	14017.16	13.27	64.22	12.27
re-TCT	14725.97	8.89	68.31	12.89
re-B-L-with loss	13927.21	13.83	63.82	12.19
re-H-C-with loss	13487.12	16.55	61.81	11.80
re-T-C-T-with loss	14068.75	12.95	65.28	12.31

There are 8.89% mismatch losses in the T-C-T reconfiguration by considering wiring losses. The 12.31% highest efficiency was obtained by the reconfigured T-C-T with wiring losses.

F. Diagonal Shading (D)

In D shading, the group of diagonal modules are shaded. Therefore, this type of shading is called diagonal shading. Twenty one groups of modules are shaded with 0.1 kW/m² and the remaining sixty groups of modules are shaded with 1 kW/m² as shown in Fig. 15. The PV curves of the T-C-T, B-L, H-C configurations and reconfigurations under Diagonal shading are shown in Fig. 16. From the results, it can be observed that highest GMP of 10,553.95 W was generated by the reconfigured T-C-T by considering wiring losses (column wiring resistance and cross ties resistance losses). It can be observed from Table VI that the T-C-T configuration has 1,033.88 W and 1,032.43 W enhancements in generated power when compared to the B-L and H-C configurations. The reconfigured T-C-T has 1,471.36 W and 659.99 W improvement in generated power than the reconfigured B-L and H-C configurations. The reconfigured T-C-T, along with wiring losses, has 1,453.36 W and 773.92 W improvements in generated

power than the reconfigured B-L and H-C configurations. Therefore, wiring losses in the reconfigured B-L, H-C, T-C-T are 305.22 W, 437.15 W, and 323.22 W respectively. The reconfigured T-C-T has the least mismatch losses of 34.7% without considering wiring losses. There are 32.7% mismatch losses in the T-C-T reconfiguration when considering wiring losses. The 9.24% highest efficiency was obtained by the reconfigured T-C-T with wiring losses.

V. CONCLUSION

In this paper, the Modified Sudoku reconfiguration is applied to 9 × 9 PV array configurations (B-L, H-C, and T-C-T) by considering cross ties resistance and column wiring resistance. The performance of PV array configurations under various shading patterns, such as short narrow, short wide, long narrow, long wide, middle, and diagonal shadings are analyzed with performance measures, such as GMP, mismatch losses, fill factor, efficiency, and P-V curves. From the results, it can be observed that the T-C-T configuration generated the highest GMP compared to B-L and H-C configurations under all shadings. The reconfigured T-C-T PV array generated the highest GMP under all considered shadings. The power enhancement in the reconfigured T-C-T with wiring losses is high when compared to reconfigured B-L and H-C configurations. But wiring losses are more in the T-C-T reconfiguration due to the greater number of cross ties. Under short narrow shading, the H-C configuration has more GMP compared to B-L. The reconfiguration of the H-C PV array generates more power compared to the reconfigured B-L PV array under long wide, diagonal shadings. In short narrow shadings, wiring losses (including both column wiring and cross ties) are greater in the reconfigured PV array configurations because a lesser number of modules are shaded. Therefore, the reconfiguration of the PV array has more effectiveness when a greater number of modules are shaded.

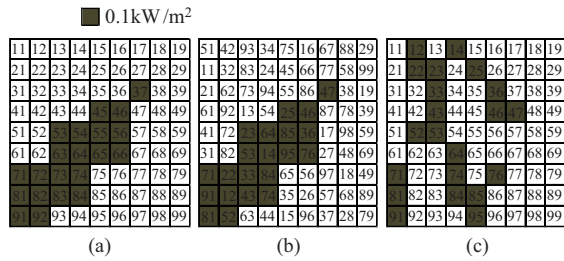


Fig. 15. Diagonal shading on: (a) 9 × 9 PV array, (b) Reconfigured 9 × 9 PV array, and (c) Shading dispersion by Sudoku.

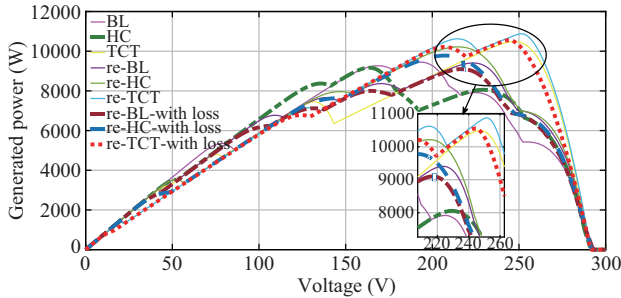


Fig. 16. Comparison of PV curves of T-C-T, B-L, H-C configuration, and reconfigurations under diagonal shading.

TABLE VII
PERFORMANCE ANALYSIS SPECIFICATIONS UNDER D SHADING

Configurations	P_{mp}	ML (%)	FF (%)	η (%)
B-L	9454.46	41.50	43.70	8.27
H-C	9167.91	43.28	42.38	8.02
T-C-T	10488.34	35.11	48.60	9.18
re-BL	9405.81	41.80	43.33	8.23
re-HC	10217.18	36.78	47.18	8.94
re-TCT	10877.17	32.70	50.40	9.52
re-B-L-with loss	9100.59	43.69	41.98	7.96
re-H-C-with loss	9780.03	39.49	45.16	8.56
re-T-C-T-with loss	10553.95	34.70	48.92	9.24

REFERENCES

- [1] A. Mohapatra, B. Nayak, P. Das, and K. B. Mohanty, "A review on MPPT techniques of PV system under partial shading condition," *Renewable and Sustainable Energy Reviews*, vol. 80, pp. 854–867, Dec. 2017.
- [2] Q. Wang and Y. Liu, "India's renewable energy: New insights from multi-regional input output and structural decomposition analysis," *Journal of Cleaner Production*, vol. 283, pp. 124230, Feb. 2021.
- [3] N. A. Lee, "Solar Energy Conversion," *Green Chemistry*, pp. 881–918, Jan. 2018.
- [4] International Energy Agency (IEA), "Snapshot of Global PV Markets 2016; Technical Report," *International Energy Agency: Paris, France*, 2017.
- [5] Y. H. Ji, D. Y. Jung, J. G. Kim, J. H. Kim, T. W. Lee, and C. Y. Won, "A real maximum power point tracking method for mismatching compensation in PV array under partially shaded conditions," *IEEE Transactions on Power Electronics*, vol. 26, no. 4, pp. 1001–1009, Apr. 2011.
- [6] D. Pilakkat and S. Kanthalakshmi, "An improved P&O algorithm integrated with artificial bee colony for photovoltaic systems under partial shading conditions," *Solar Energy*, vol. 178, pp. 37–47, Jan. 2019.
- [7] E. Koutroulis and F. Blaabjerg, "A new technique for tracking the global maximum power point of PV arrays operating under partial-shading conditions," *IEEE Journal of Photovoltaics*, vol. 2, no. 2, pp. 184–190, Apr. 2012.
- [8] M. Dhimish, "Assessing MPPT techniques on hot-spotted and partially shaded photovoltaic modules: comprehensive review based on experimental data," *IEEE Transactions on Electron Devices*, vol. 66, no. 3, pp. 1132–1144, Mar. 2019.

- [9] E. V. Paraskevadaki and S. A. Papatthanassiou, "Evaluation of MPP voltage and power of mc-Si PV modules in partial shading conditions," *IEEE Transactions on Energy Conversion*, vol. 26, no. 3, pp. 923–932, Sep. 2011.
- [10] A. O. Baba, G. Y. Liu, and X. H. Chen, "Classification and evaluation review of maximum power point tracking methods," *Sustainable Futures*, vol. 2, pp. 100020, Apr. 2020.
- [11] E. Karatepe, M. Boztepe, and M. Çolak, "Development of a suitable model for characterizing photovoltaic arrays with shaded solar cells," *Solar Energy*, vol. 81, no. 8, pp. 977–992, Aug. 2007.
- [12] Y. J. Wang and P. C. Hsu, "An investigation on partial shading of PV modules with different connection configurations of PV cells," *Energy*, vol. 36, no. 5, pp. 3069–3078, May 2011.
- [13] S. R. Pendem and S. Mikkili, "Modeling, simulation, and performance analysis of PV array configurations (Series, Series-Parallel, Bridge-Linked, and Honey-Comb) to harvest maximum power under various Partial Shading Conditions," *International Journal of Green Energy*, vol. 15, no. 13, pp. 795–812, Oct. 2018.
- [14] S. R. Pendem and S. Mikkili, "Modelling and performance assessment of PV array topologies under partial shading conditions to mitigate the mismatching power losses," *Solar Energy*, vol. 160, pp. 303–321, Jan. 2018.
- [15] N. D. Kaushika and N. K. Gautam, "Energy yield simulations of interconnected solar PV arrays," in *2003 IEEE Power Engineering Society General Meeting (IEEE Cat. No.03CH37491)*, Toronto, 2003, pp. 2618.
- [16] A. Mäki and S. Valkealahti, "Effect of photovoltaic generator components on the number of MPPs under partial shading conditions," *IEEE Transactions on Energy Conversion*, vol. 28, no. 4, pp. 1008–1017, Dec. 2013.
- [17] R. Ramaprabha and B. L. Mathur, "A comprehensive review and analysis of solar photovoltaic array configurations under partial shaded conditions," *International Journal of Photoenergy*, vol. 2012, pp. 120214, Mar. 2012.
- [18] T. Ramesh, K. Rajani, and A. K. Panda, "A novel triple-tied-cross-linked PV array configuration with reduced number of cross-ties to extract maximum power under partial shading conditions," *CSEE Journal of Power and Energy Systems*, vol. 7, no. 3, pp. 567–581, May 2021.
- [19] P. K. Bonthagorla and S. Mikkili, "A novel fixed PV array configuration for harvesting maximum power from shaded modules by reducing the number of cross-ties," *IEEE Journal of Emerging and Selected Topics in Power Electronics*, vol. 9, no. 2, pp. 2109–2121, Apr. 2021.
- [20] A. A. Desai and S. Mikkili, "Modelling and analysis of PV configurations (alternate TCT-BL, total cross tied, series, series parallel, bridge linked and honey comb) to extract maximum power under partial shading conditions," *CSEE Journal of Power and Energy Systems*, doi: 10.17775/CSEEJPES.2020.00900.
- [21] D. P. Winston, S. Kumaravel, B. P. Kumar, and S. Devakirubakaran, "Performance improvement of solar PV array topologies during various partial shading conditions," *Solar Energy*, vol. 196, pp. 228–242, Jan. 2020.
- [22] A. Bidram, A. Davoudi, and R. S. Balog, "Control and circuit techniques to mitigate partial shading effects in photovoltaic arrays," *IEEE Journal of Photovoltaics*, vol. 2, no. 4, pp. 532–546, Oct. 2012.
- [23] S. Busquets-Monge, J. Rocabert, P. Rodriguez, S. Alepuz, and J. Bordonau, "Multilevel diode-clamped converter for photovoltaic generators with independent voltage control of each solar array," *IEEE Transactions on Industrial Electronics*, vol. 55, no. 7, pp. 2713–2723, Jul. 2008.
- [24] E. Karatepe, T. Hiyama, M. Boztepe, and M. Colak, "Power controller design for photovoltaic generation system under partially shaded insolation conditions," in *2007 International Conference on Intelligent Systems Applications to Power Systems*, Kaohsiung, China, 2007, pp. 1–6.
- [25] G. Spagnuolo, G. Petrone, B. Lehman, C. A. R. Paja, Y. Zhao, and M. L. O. Gutierrez, "Control of photovoltaic arrays: dynamical reconfiguration for fighting mismatched conditions and meeting load requests," *IEEE Industrial Electronics Magazine*, vol. 9, no. 1, pp. 62–76, Mar. 2015.
- [26] K. Ş. Parlak, "PV array reconfiguration method under partial shading conditions," *International Journal of Electrical Power & Energy Systems*, vol. 63, pp. 713–721, Dec. 2014.
- [27] K. H. Chao, P. L. Lai, and B. J. Liao, "The optimal configuration of photovoltaic module arrays based on adaptive switching controls," *Energy Conversion and Management*, vol. 100, pp. 157–167, Aug. 2015.
- [28] A. Tabanjat, M. Becherif, and D. Hissel, "Reconfiguration solution for shaded PV panels using switching control," *Renewable Energy*, vol. 82, pp. 4–13, Oct. 2015.
- [29] B. I. Rani, G. S. Ilango, and C. Nagamani, "Enhanced power generation from PV array under partial shading conditions by shade dispersion using Su Do Ku configuration," *IEEE Transactions on Sustainable Energy*, vol. 4, no. 3, pp. 594–601, Jul. 2013.
- [30] M. Horoufiany and R. Ghandehari, "Optimization of the sudoku based reconfiguration technique for PV arrays power enhancement under mutual shading conditions," *Solar Energy*, vol. 159, pp. 1037–1046, Jan. 2018.
- [31] G. S. Krishna and T. Moger, "Improved Sudoku reconfiguration technique for total-cross-tied PV array to enhance maximum power under partial shading conditions," *Renewable and Sustainable Energy Reviews*, vol. 109, pp. 333–348, Jul. 2019.
- [32] I. Nasiruddin, S. Khatoun, M. F. Jalil, and R. C. Bansal, "Shade diffusion of partial shaded PV array by using odd-even structure," *Solar Energy*, vol. 181, pp. 519–529, Mar. 2019.
- [33] S. S. Reddy and C. Yammani, "A novel magic-square puzzle based one-time PV reconfiguration technique to mitigate mismatch power loss under various partial shading conditions," *Optik*, vol. 222, pp. 165289, Nov. 2020.
- [34] G. Sagar, D. Pathak, P. Gaur, and V. Jain, "A Su Do Ku puzzle based shade dispersion for maximum power enhancement of partially shaded hybrid bridge-link-total-cross-tied PV array," *Solar Energy*, vol. 204, pp. 161–180, Jul. 2020.
- [35] S. Vijayalekshmy, G. R. Bindu, and S. R. Iyer, "A novel zig-zag scheme for power enhancement of partially shaded solar arrays," *Solar Energy*, vol. 135, pp. 92–102, Oct. 2016.
- [36] K. Rajani and T. Ramesh, "Maximum power enhancement under partial shadings using a modified Sudoku reconfiguration," *CSEE Journal of Power and Energy Systems*, vol. 7, no. 6, pp. 1187–1201, Jul. 2021.
- [37] Y. A. Mahmoud, W. D. Xiao, and H. H. Zeineldin, "A parameterization approach for enhancing PV model accuracy," *IEEE Transactions on Industrial Electronics*, vol. 60, no. 12, pp. 5708–5716, Dec. 2013.
- [38] M. G. Villalva, J. R. Gazoli, and E. R. Filho, "Comprehensive approach to modeling and simulation of photovoltaic arrays," *IEEE Transactions on Power Electronics*, vol. 24, no. 5, pp. 1198–1208, May 2009.
- [39] D. Job and V. Paul, "Recursive backtracking for solving 9*9 sudoku puzzle," *Bonfring International Journal of Data Mining*, vol. 6, no. 1, pp. 7–9, Jan. 2016.
- [40] J. Wiles, "Photovoltaic power systems and the national electrical code: suggested practices," US Department of Energy, Washington, SAND2001–0674, Mar. 2001.
- [41] CED Greentech. (2020). Determining Module Inter-Row Spacing. [Online]. <http://cedgreentech.com/article/determining-module-inter-row-spacing>.
- [42] R. B. Bollipo, S. Mikkili and P. K. Bonthagorla, "Hybrid, optimal, intelligent and classical PV MPPT techniques: A review," *CSEE Journal of Power and Energy Systems*, vol. 7, no. 1, pp. 9–33, Jan. 2021.
- [43] S. Wang, "Current status of PV in China and its future forecast," *CSEE Journal of Power and Energy Systems*, vol. 6, no. 1, pp. 72–82, Mar. 2020, doi: 10.17775/CSEEJPES.2019.03170.



energy sources, control systems and power electronics.



power electronics and drives, electrical machines, applications of soft computing techniques, and renewable energy sources. He has reported the results of his research (25+ papers) in international journals and conferences.

Kandipati Rajani graduated in Electrical and Electronics Engineering from JNTU Kakinada. She did her M.E (Control Systems) in the Electrical Engineering Department of Andhra University. Currently, she is pursuing a Ph.D. degree in the Electrical Engineering Department, National Institute of Technology, Andhra Pradesh, and also working as an Assistant Professor for the Electrical and Electronics Engineering Department, Vignana's Lara Institute of Technology & Sciences, Guntur, Andhra Pradesh, India. Her research interests include renewable energy

Tejavathu Ramesh received a B.Tech. degree in Electrical and Electronics Engineering from JNTU Hyderabad, India, in 2009. He received M.Tech. and Ph.D. degrees in Electrical Engineering from the National Institute of Technology, Rourkela, India, in 2011 and 2016, respectively. He is currently an Assistant Professor in the Department of Electrical Engineering at National Institute of Technology Andhra Pradesh, India. Since, 2019, he has been the Deputy Registrar of the Hostels & Guest House at NIT Andhra Pradesh. His research interests include